Fabrication and luminescence properties in Yb –Tb co-doped a-SiCO thin films

Loreleyn F Flores[1]*, Karem Y Tucto[1], Jorge A Guerra[1], Rolf Grieseler[1,3], Jan A Töfflinger[1], Andres Osvet[2], Miroslaw Batentschuk[2], Roland Weingärtner[1]

[1]Departamento de Ciencias, Sección Física, Pontificia Universidad Católica del Perú, Av. Universitaria 1801, Lima 32, Perú
[2]Department of Material Science 6, University of Erlangen-Nuremberg, Martenstr. 6, Erlangen 91058, Germany
[3]Chair Materials for Electronics, Institute of Materials Engineering and Institute of Micro and Nanotechnologies MacroNano, TU Ilmenau, Gustav-Kirchhoff-Str. 5, 98693 Ilmenau, Germany

*Corresponding author

DOI: 10.5185/amp2018/411
www.vbripress.com/amp

Abstract

Amorphous silicon oxycarbide (a-SiC_xO_y) single doped with Yb^{3+} and co-doped with the couple Tb^{3+} - Yb^{3+} thin films were grown on crystalline silicon substrates by rf magnetron sputtering. The elemental composition in at. % is determined by energy dispersive spectroscopy and fourier transform infrared spectroscopy allows to investigate the chemical properties of the host. The concentration of Yb in the single doped sample was 3.5% and for the codoped samples (Yb, Tb) were (3%, 0.9%), (3.5%, 0.6%) and (4%, 0.6%), respectively. Post-deposition annealing treatments were made in order to induce optical activation of the rare earths. Conversion or absorption of high energy photons were analyzed by photoluminescence spectroscopy. The photoluminescence spectra show that for a given temperature range in the thermal annealing process, as well as for the appropriate rare earth concentrations the activation of Yb^{3+} and Tb^{3+} is enhanced. A strong reduction of the Tb^{3+} emission in contrast to the Yb^{3+} emission in the a-SiC_xO_y,:Tb:Yb samples at annealing temperature at 500°C suggests a energy transfer from Tb^{3+} to Yb^{3+} ions. Copyright © 2018 VBRI Press.

Keywords: Energy transfer, silicon oxycarbide, photoluminescence.

Introduction

The applications of rare earths (RE) in different technologies are increasing, especially in renewable energy sources such as photovoltaics. The main limiting in the conversion efficiency of solar energy to electricity is caused by the so-called spectral mismatch. Loss mechanisms lead that low energy photons are not absorbed by a solar cell while high energy photons are not used efficiently **[1,2]**. The use of rare earths offer an approach to improve the solar cells efficiency through the application of spectral converters, i.e. up- and down-conversion (UC and DC) are viable options. In the case of upconverters two or more low energy photons which cannot be absorbed by the solar cell, are added up to give one high energy photon which can be absorbed **[3,4]**. In the same way for the case of quantum cutting or down-conversion one high energy is absorbed to emit two or more lower energy photons which can be absorbed by the solar cell **[5–7]**.

Among different RE systems for DC applicable for crystalline silicon based solar cell those who use Yb^{3+} ions seem to be promising. The Yb^{3+} ions have a transition from the $^2F_{5/2}$ to the $^2F_{7/2}$ energy level, corresponding to energy of 1.26 eV (980nm) just above the crystalline silicon band gap of 1.1 eV and as a consequence diminish the thermalization in these solar cells. The couple of Tb^{3+} -Yb^{3+} is suitable due to the Tb^{3+} ions have a transition from the $^5D_4$ to the $^6F_7$ energy level corresponding to energy of 2.53 eV (490nm) which is twice of energy transition of Yb^{3+} ions. These systems allow the absorption of UV photons by Tb^{3+} ions and have the potential to transfer the energy to two neighboring Yb^{3+} ions by means of cooperative energy transfer **[8,9]**.

In order to enhance the down-conversion properties a suitable host has to be found, i.e. which maximizes rare earth activation, the energy transfer between the rare earth couple and minimize quenching effects. Different hosts like phosphors **[10,11]**, oxyfluoride glass **[12]**, tellurite glass **[13]**, silicon oxynitride **[14]**, aluminum oxynitride **[15]** and silicon nitride thin films **[9]** among other were reported. The amorphous silicon oxycarbide (a-SiCO) refers a kind of glassy compound materials consisting of Si, C, and O atoms, specifically to a carbon-containing silicate glass where in oxygen and carbon atoms share bonds with silicon in the amorphous structure **[16,17]**. Also Si-based matrices are compatible with silicon solar cell fabrication process. In addition, silicon oxycarbide SiCO offers flexibility in his refractive index which can be tuned between SiO_2 (1.45) and a-SiC (3.2) **[18]**, condition that would allow as spectral

converter layers (UC or DC) with a suitable refractive index to optimize the efficiency of the solar cells. Silicon oxycarbide has a broad spectral range, from the ultraviolet, to visible **[19]**. In the literature previous work reported that its strong light emission can be tuned from yellow to blue by modulating the oxygen content in the films **[20]**. Also in other matrix (a-Si_{1-x} C_x: H) is found that by varying the carbon content, high luminescence efficiencies are achieved **[21]**. It has also been evidenced that SiCO is a promising host material to activate optically rare earth ions. This host has been reported in studies of europium (Eu^{2+}) - doped **[22,23]**, as well as in studies of erbium (Er^{3+}) - doped SiCO **[24–26]**.

In this work silicon oxycarbide doped with Yb^{3+} and co-doped with Tb^{3+} - Yb^{3+} thin films were grown onto silicon substrates using rf magnetron sputtering. In order to investigate chemical properties of the host, elemental composition by energy dispersive spectroscopy (EDS) and fourier transform infrared spectroscopy (FT-IR) were analyzed. Photoluminescence spectroscopy (PL) allowed studying the conversion or absorption of high energy photons. Finally, sequential annealing treatments up to 850°C reveals the photoluminescence behavior of the Yb^{3+} and Tb^{3+} emission and suggest energy transfer from the Tb^{3+} to the Yb^{3+} ions.

Experimental

Materials and sample preparation

Amorphous silicon oxycarbide doped with Yb^{3+} and co-doped with Tb^{3+}-Yb^{3+} thin films were grown using rf magnetron sputtering **[27]**. Three disks of 51 mm diameter and high purity SiC (main impurity: nitrogen less than 10 ppm wt **[28]**), Tb and Yb (3N of purity) were used as targets. These targets were sputtered simultaneously at appropriate rf powers (110 W for SiC, 15W for Yb and 10W for Tb). The base pressure was 3.5×10^{-6} mbar. The deposition process was performed in a nitrogen, argon and oxygen mixture atmosphere of purity 5N, respectively. Film thicknesses of 300nm have been obtained. Polished crystalline silicon wafers were used as substrates and kept cooled during the deposition process below 100 °C to ensure the amorphous state of the grown films.

Annealing process

After the deposition of Yb^{3+} and Tb^{3+} - Yb^{3+} co-doped SiCO thin films, post-deposition annealing treatments were made and took place in a quartz tube furnace from 150 ºC up to 850 ºC in steps of 50/100 °C and maintained for 35 min under argon atmosphere to prevent oxygen diffusion. The annealing process is perform in such a way to achieve fastest heating and cooling rates, i.e. the samples are moved in rapidly into the preheated furnace. After each annealing treatment the samples were immediately removed from the furnace and natural cooling were carried out. The same samples were used for the next annealing steps. These process has shown to achieve maximal rare earth activation **[29]**.

Characterizations

The elemental composition of the samples and the approximate concentration of each element was determined using a scanning electron microscope (FEI Quanta 650) equipped with a tungsten filament gun and a concentric backscatter detector for EDS. A beam voltage of 5 kV was applied in order to achieve small electron penetration in the sample and in this way to reduce the contribution of the silicon substrate in the measurement. Bond related vibrational modes were obtained by FT-IR in the range from 400 cm^{-1} to 4000 cm^{-1} using a Perkin Elmer FTIR spectrometer model Spectrum 1000. The substrates were also measured to be taken into account for corrections.

The optical emission was performed through photoluminescence measurements. The PL spectra were recorded with a Ranishaw inVia Reflex spectrometer system for Raman and PL spectroscopy. He-Cd laser at 325 nm was used as an excitation source. All measurements were performed at room temperature.

Results and discussion

The elemental atomic concentrations of the as-deposited samples are summarized in **Table 1. Fig. 1** presents the FT-IR absorption spectra of SiOC films. The IR spectra of a-SiCO from 400 to 1600 cm^{-1} exhibited a rocking mode of Si-O-Si bonds at 437 cm^{-1}, while a broad region with Si-C and Si-O bonds were seen in the 600–1400 cm^{-1} range **[30]** which verifies the formation of silicon oxycarbide.

Table 1. Elemental composition (at.%).

	SiC_xO_y:Yb^{3+}	SiC_xO_y : Tb^{3+}-Yb^{3+}		
C	20.7	11.2	10.9	9.4
O	47.0	52.2	50.2	50.3
Tb	-	0.6	0.6	0.9
Yb	3.5	4.0	3.5	3.0
Si	28.6	31.9	34.8	36.5

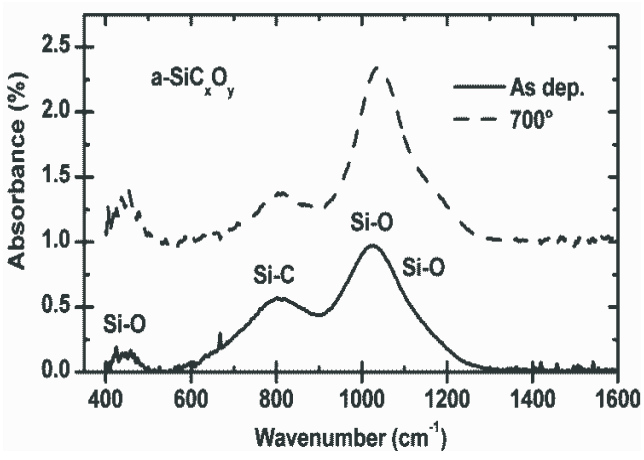

Fig. 1. FT-IR spectra measured of a-SiCO layers grown on *c*-Si (100) substrate.

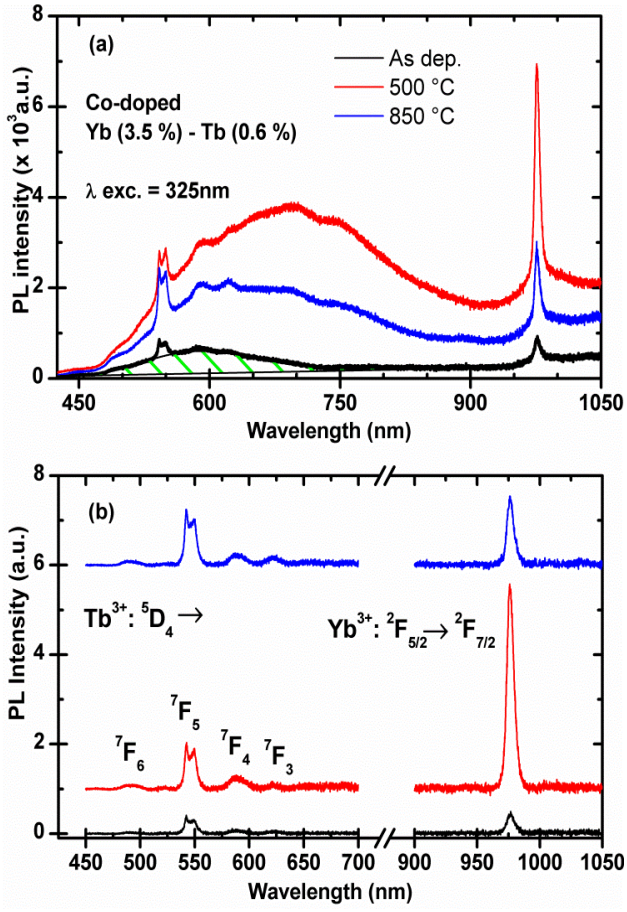

Fig. 2. (a) PL emission spectra of a-SiCO:Tb^{3+}:Yb^{3+} for as deposited and post-annealing treatments at 500 °C and 850 °C upon excitation of 325 nm at room temperature. Values in parenthesis indicate dopant concentrations in atomic percentage (at.%). (b) Same PL emission spectra with background correction (host) as in (a) and artificial baseline shift for better visualization.

The emission spectra of a-SiCO:Tb^{3+}:Yb^{3+} thin films for different post annealing treatments under laser excitation of 325nm are shown in **Fig. 2 (a).** These PL spectra show a broad emission (dashed pattern) due to unknown defect state of the a-SiCO host and the typical emission spectra of the Tb3+ and Yb^{3+} ions. The emission in the region Vis-NIR was assigned for transition energy levels of Tb^{3+}, 490 nm ($^5D_4 \rightarrow {}^7F_6$), 545 nm ($^5D_4 \rightarrow {}^7F_5$), 588 nm ($^5D_4 \rightarrow {}^7F_4$) and 621 nm ($^5D_4 \rightarrow {}^7F_3$) and 980nm ($^2F_{5/2} \rightarrow {}^2F_{7/2}$) transition between energy levels of Yb^{3+}. The emission of the host will be considered for the study of the effect of post annealing treatments in the luminescence emission of the couple Tb-Yb. In order to investigate the role of energy transfer between Yb^{3+} and Tb^{3+} in **Fig. 2 (b)** the PL spectra of the host was substrated from the PL spectra of the Yb/Tb couple ions.

Fig. 3. (a) shows the activation curve corresponding to the behavior of the transition of Yb^{3+} (980nm) (b) shows three activation curves corresponding to the behavior of the dominating transition of Tb^{3+} (545nm), the transition of Yb^{3+} (980nm) and also the emission of the host (broad band 450-900nm). Regarding of the luminescence behavior for Yb^{3+} single doped-and Yb^{3+} co-doped samples two regions related with post annealing treatments can be identified. First the activation region until 550 °C which correspond to the activation of new Yb^{3+} ions increasing the PL emission intensity. Second, deactivation or quenching region after 550 °C which corresponds to the competition between recombination in non – radiative channels (correlated to the defect density of the host) and the emission of new activated luminescent centers **[31,32]**. Concerning the behavior of the host related emission in Tb^{3+}-Yb^{3+} co-doped samples, the effect of thermal annealing on the PL of a-SiCO is the same as obtained in the work of Lin, et al. **[33]**, suggesting that this emission is correlated to Si-C-O bonds.

Finally, one would expect a similar behavior for the Tb^{3+} emission spectra, in the absence of energy transfer between the Tb-Yb couple. Previous works have shown the temperature activation of Tb^{3+} singly doped a-SiC matrix occurs up to 600°C **[31,32]**. However in case of Tb^{3+} in a co-doped sample with Yb^{3+} is observed again the activation region (from As deposited to 350 °C), the quenching region (above 650 °C), as well a region between 350 and 650 ° C where the deactivating of the radiative transitions of Tb^{3+} occur in favor of the emission of Yb^{3+} ions.

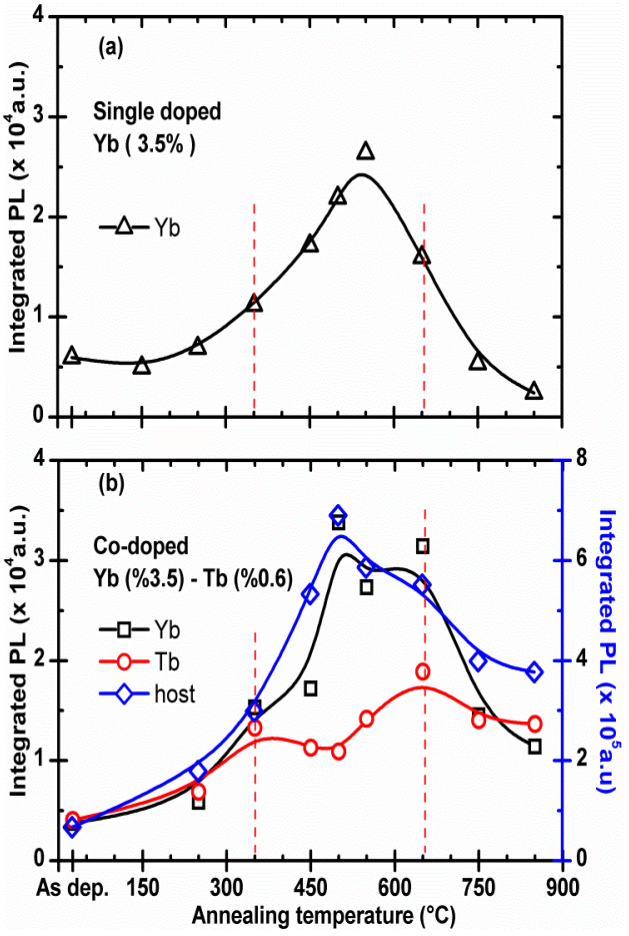

Fig. 3. (a) Integrated PL intensities of the transition of Yb^{3+} (980nm) (b) Integrated PL intensities of the main transition of Tb^{3+} (545nm), Yb^{3+} (980nm) and also integrated intensity of broad band (450-900nm) corresponding to emission of the host, as a function of annealing temperature.

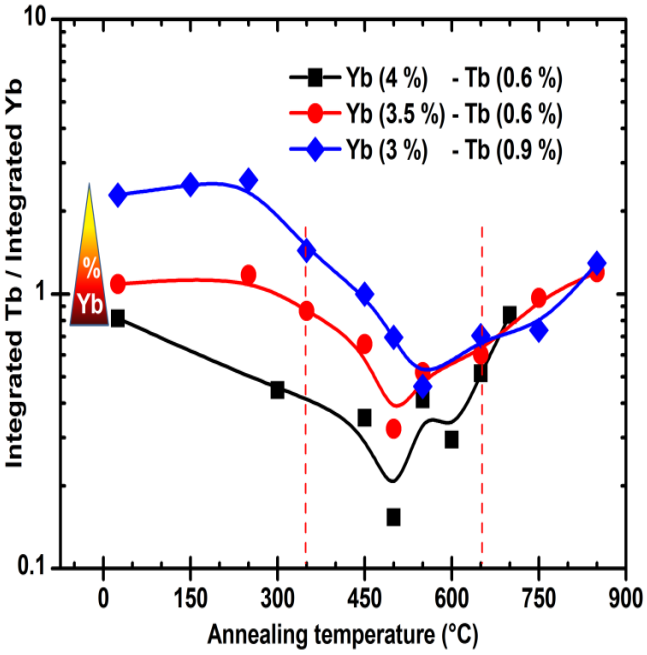

Fig. 4. Tb^{3+}/Yb^{3+} ratio of the integrated PL intensities of the main transitions as a function of the annealing temperature for different co-doped atomic concentration. The values in parenthesis indicate dopant concentrations in atomic percentage (at.%).

For a better appreciation of the annealing effect on the luminescence of Tb^{3+} and Yb^{3+} ions in co-doped samples, and also to separate the emission of the matrix we show in Fig. 4 the ratio of the integrated intensities of Tb^{3+}/Yb^{+3} as a function of temperature. In this graph the intensity of both rare earths can be compared, the annealing behavior remains similar up to 250 °C indicating a constant activation of both Tb^{3+} and Yb^{3+} ions. From 350 °C on there is a suppression in the emission of the Tb^{3+} compared to the Yb^{3+} until reaching a minimum at 500 °C. The last behavior can be associated with the maximum energy transfer from Tb^{3+} to Yb^{3+} at this annealing temperature. Also **Fig. 4** compares the effect of thermal treatment for different concentrations of the couple Tb-Yb. The ratio of the integrated intensity Tb^{3+}/Yb^{3+} is shown for three different concentrations of co-dopants, indicating a high concentration of Yb and a low concentration of Tb. Atomic ratio between the couple of Tb-Yb ions are of about 3 to 6. These doping relations have been applied intentionally in order to have sufficient Yb^{3+} ions in the surrounding of the Tb^{3+} ions and therefore promote the cooperative energy transfer between them.

The luminescence behaviors of the Tb^{3+} ions with different concentrations of co-doped samples have the same tendency. In all cases the region of suppression of the Tb^{3+} spectra is observed, having a smaller emission around 500 °C. This behavior is expected if an energy transfer process from Tb^{3+} to Yb^{3+} occurs. In addition, the increase in the concentrations of Yb^{3+} in the co-doped samples leads to a lower Tb^{3+} emission intensity, which also would support the energy transfer possibility from Tb^{3+} to Yb^{3+} ions.

Conclusion

This work reports the results obtained for the PL emission properties of a-SiCO:Yb^{3+} and a-SiCO:Tb^{3+}:Yb^{3+} thin films produced by radiofrequency magnetron sputtering. The post annealing treatment of the samples were performed at different annealing temperatures from 150 to 850 °C in steps of 50/100 °C. The photoluminescence spectra of the co-doped Tb^{3+} and Yb^{3+} system show that for a given temperature range in the thermal annealing process, as well as for the appropriate rare earth concentrations the activation of Yb^{3+} and Tb^{3+} is enhanced. A strong reduction of the Tb^{3+} emission in contrast to the Yb^{3+} emission, suggest a energy transfer from Tb^{3+} to Yb^{3+} ions.

Acknowledgements

We acknowledge the financial support of the Peruvian science foundation Cienciactiva in the framework of the DAAD-CONCYTEC joint project (2017-2019), the "Círculo de investigación" (1181-2014) project and the Research Management Office (DGI ID492) of the Pontificia Universidad Católica del Perú. The research activity was performed in the framework of the doctoral scholarship of L. Flores and K. Tucto from CONCYTEC under the contract numbers 000236-2015-FONDECYT-DE and 012-2013-FONDECYT, respectively. The authors are also grateful to the Center of Microcharacterization of the PUCP for the EDX and PL measurements.

References

1. Van der Ende, B. M.; Aarts, L.; Meijerink, A. *Phys. Chem. Chem. Phys.* **2009**, *11* (47), 11081. **DOI:** 10.1039/b913877c
2. Huang, X.; Han, S.; Huang, W.; Liu, X. *Chem. Soc. Rev.* **2013**, *42* (1), 173. **DOI:** 10.1039/c2cs35288e
3. Dong, H.; Sun, L. D.; Yan, C. H. *Chem Soc Rev* **2015**, *44* (6), 1608. **DOI:** 10.1039/c4cs00188e
4. Wang, H. Q.; Batentschuk, M.; Osvet, A.; Pinna, L.; Brabec, C. J. *Adv. Mater.* **2011**, *23* (22–23), 2675. **DOI:** 10.1002/adma.201100511
5. Richards, B. S. *Sol. Energy Mater. Sol. Cells* **2006**, *90* (9), 1189. **DOI:** 10.1016/j.solmat.2005.07.001
6. Richards, B. S. *Sol. Energy Mater. Sol. Cells* **2006**, *90* (15), 2329. **DOI:** 10.1016/j.solmat.2006.03.035
7. De la Mora, M. B.; Amelines-Sarria, O.; Monroy, B. M.; Hernández-Pérez, C. D.; Lugo, J. E. *Sol. Energy Mater. Sol. Cells* **2017**, *165* (January), 59. **DOI:** 10.1016/j.solmat.2017.02.016
8. Fu, L.; Xia, H.; Dong, Y.; Li, S.; Jiang, H.; Chen, B. *IEEE Photonics J.* **2014**, *6* (1). **DOI:** 10.1109/JPHOT.2014.2300495
9. Dumont, L.; Cardin, J.; Benzo, P.; Carrada, M.; Labbé, C.; Richard, A. L.; Ingram, D. C.; Jadwisienczak, W. M.; Gourbilleau, F. *Sol. Energy Mater. Sol. Cells* **2016**, *145*, 84. **DOI:** 10.1016/j.solmat.2015.09.031
10. Yuan, J.-L.; Zeng, X.-Y.; Zhao, J.-T.; Zhang, Z.-J.; Chen, H.-H.; Yang, X.-X. *J. Phys. D. Appl. Phys.* **2008**, *41* (10), 105406. **DOI:** 10.1088/0022-3727/41/10/105406
11. Huang, X. Y.; Zhang, Q. Y. *J. Appl. Phys.* **2009**, *105* (5), 5. **DOI:** 10.1063/1.3088890
12. Duan, Q.; Qin, F.; Wang, D.; Xu, W.; Cheng, J.; Zhang, Z.; Cao, W. *J. Appl. Phys.* **2011**, *110* (11), 1. **DOI:** 10.1063/1.3662916
13. Florêncio, L. de A.; Gómez-Malagón, L. A.; Lima, B. C.; Gomes, A. S. L.; Garcia, J. A. M.; Kassab, L. R. P. *Sol. Energy Mater. Sol. Cells* **2016**, *157*, 468. **DOI:** 10.1016/j.solmat.2016.07.024
14. An, Y.-T.; Labbé, C.; Cardin, J.; Morales, M.; Gourbilleau, F. *Adv. Opt. Mater.* **2013**, *1* (11), 855. **DOI:** 10.1002/adom.201300186

15. Tucto, K.; Flores, L.; Guerra, J.; Töfflinger, J.; Dulanto, J.; Grieseler, R.; Osvet, A.; Batentschuk, M.; Weingärtner, R. *MRS Adv. © 2017 Mater. Res. Soc.* **2017**, *3*, 4, **DOI:** 10.1557/adv.2017
16. Pantano, C. G.; Pantano, C. G.; Singh, A. K.; Singh, A. K.; Zhang, H.; Zhang, H. *J. Sol-Gel Sci. Technol.* **1999**, *14*, 7. **DOI:** 10.1023/A:1008765829012
17. Shevchuk, S. L.; Maishev, Y. P. *Thin Solid Films* **2005**, *492* (1–2), 114. **DOI:** 10.1016/j.tsf.2005.06.086
18. Memon, F. A.; Morichetti, F.; Abro, M. I.; Iseni, G.; Somaschini, C.; Aftab, U.; Melloni, A. *EPJ Web Conf.* **2017**, *139*, 0. **DOI:** 10.1051/epjconf/201713900002
19. Nikas, V.; Gallis, S.; Huang, M.; Kaloyeros, A. E.; Nguyen, A. P. D.; Stesmans, A.; Afanas'Ev, V. V. *Appl. Phys. Lett.* **2014**, *104* (6), 6. **DOI:** 10.1063/1.4865100
20. Lin, Z.; Guo, Y.; Song, C.; Song, J.; Wang, X.; Zhang, Y.; Huang, R.; Huang, X. *J. Alloys Compd.* **2015**, *633*, 153. **DOI:** 10.1016/j.jallcom.2015.02.027
21. Tessler, L. R.; Solomon, I. *Phys. Rev. B* **1995**, *52* (15), 10962. **DOI:** 10.1103/PhysRevB.52.10962
22. Boninelli, S.; Bellocchi, G.; Franzò, G.; Miritello, M.; Iacona, F. *J. Appl. Phys.* **2013**, *113* (14). **DOI:** 10.1063/1.4799407
23. Bellocchi, G.; Franzò, G.; Boninelli, S.; Miritello, M.; Cesca, T.; Iacona, F.; Priolo, F. *IOP Conf. Ser. Mater. Sci. Eng.* **2014**, *56*, 12009. **DOI:** 10.1088/1757-899X/56/1/012009
24. Gallis, S.; Huang, M.; Efstathiadis, H.; Eisenbraun, E.; Kaloyeros, A. E.; Nyein, E. E.; Hommerich, U. *Appl. Phys. Lett.* **2005**, *87* (9), 7. **DOI:** 10.1063/1.2032600
25. Gallis, S.; Huang, M.; Kaloyeros, A. E. *Appl. Phys. Lett.* **2007**, *90* (16), 19. **DOI:** 10.1063/1.2730583
26. Nikas, V.; Gallis, S.; Huang, M.; Kaloyeros, A. E. *J. Appl. Phys.* **2011**, *109* (9). **DOI:** 10.1063/1.3582090
27. Gálvez De La Puente, G.; Guerra Torres, J. A.; Erlenbach, O.; Steidl, M.; Weingärtner, R.; De Zela, F.; Winnacker, A. *Mater. Sci. Eng. B Solid-State Mater. Adv. Technol.* **2010**, *174* (1–3), 127. **DOI:** 10.1016/j.mseb.2010.03.012
28. Bickermann, M.; Hofmann, D.; Rasp, M.; Straubinger, T. L.; Weingärtner, R.; Wellmann, P. J.; Winnacker, A. In *Materials Science Forum*; 2001; Vol. 353–356, 49.
29. Tucto Salinas, K. Y.; Flores Escalante, L. F.; Guerra Torres, J. A.; Grieseler, R.; Kups, T.; Pezoldt, J.; Osvet, A.; Batentschuk, M.; Weingärtner, R. *Mater. Sci. Forum* **2017**, *890* (Cl), 299. **DOI:** 10.4028/www.scientific.net/MSF.890.299
30. Gallis, S.; Nikas, V.; Huang, M.; Eisenbraun, E.; Kaloyeros, A. E. *J. Appl. Phys.* **2007**, *102* (2). **DOI:** 10.1063/1.2753572
31. Guerra, J. A.; De Zela, F.; Tucto, K.; Montañez, L.; Töfflinger, J. A.; Winnacker, A.; Weingärtner, R. *J. Phys. D. Appl. Phys.* **2016**, *49* (37), 375104. **DOI:** 10.1088/0022-3727/49/37/375104
32. Guerra, J. A.; Benz, F.; Zanatta, A. R.; Strunk, H. P.; Winnacker, A.; Weing??rtner, R. *Phys. Status Solidi Curr. Top. Solid State Phys.* **2013**, *10* (1), 68. **DOI:** 10.1002/pssc.201200394
33. Lin, Z.; Guo, Y.; Song, J.; Zhang, Y.; Song, C.; Wang, X.; Huang, R. *J. Non. Cryst. Solids* **2015**, *428*, 184. **DOI:** 10.1016/j.jnoncrysol.2015

